

I.16 Periodic Solutions, Limit Cycles, Strange Attractors

2^o Les demi-spirales que l'on suit sur un arc infini sans arriver à un nœud ou à un foyer et sans revenir au point de départ ; ...
(H. Poincaré 1882, Oeuvres vol. 1, p. 54)

The phenomenon of limit cycles was first described theoretically by Poincaré (1882) and Bendixson (1901), and has since then found many applications in Physics, Chemistry and Biology. In higher dimensions things can become much more chaotic and attractors may look fairly “strange”.

Van der Pol's Equation

I have a theory that whenever you want to get in trouble with a method, look for the Van der Pol equation.

(P.E. Zadunaisky 1982)

The first practical examples were studied by Rayleigh (1883) and later by Van der Pol (1920-1926) in a series of papers on nonlinear oscillations: the solutions of

$$y'' + \alpha y' + y = 0$$

are *damped* for $\alpha > 0$, and *unstable* for $\alpha < 0$. The idea is to change α (with the help of a triode, for example) so that $\alpha < 0$ for small y and $\alpha > 0$ for large y . The simplest expression, which describes the physical situation in a somewhat idealized form, would be $\alpha = \varepsilon(y^2 - 1)$, $\varepsilon > 0$. Then the above equation becomes

$$y'' + \varepsilon(y^2 - 1)y' + y = 0, \quad (16.1)$$

or, written as a system,

$$\begin{aligned} y'_1 &= y_2 \\ y'_2 &= \varepsilon(1 - y_1^2)y_2 - y_1, \quad \varepsilon > 0. \end{aligned} \quad (16.2)$$

In this equation, small oscillations are amplified and large oscillations are damped. We therefore expect the existence of a stable periodic solution to which all other solutions converge. We call this a *limit cycle* (Poincaré 1882, “Chap. VI”). The original illustrations of the paper of Van der Pol are reproduced in Fig. 16.1.

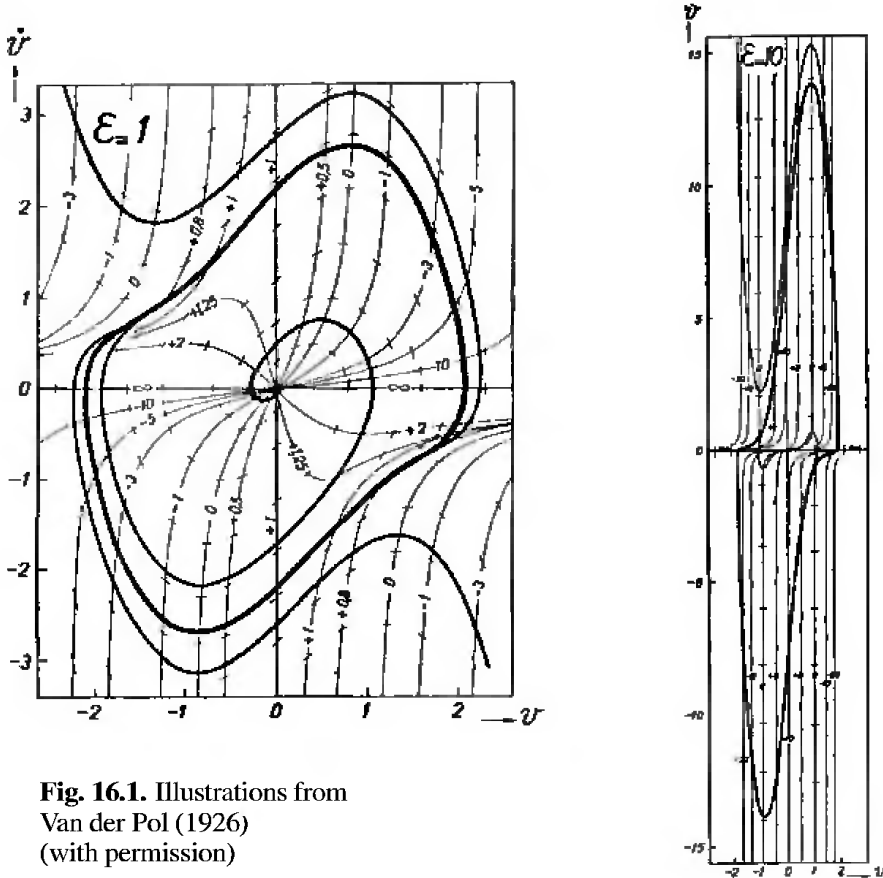


Fig. 16.1. Illustrations from
Van der Pol (1926)
(with permission)

Existence proof. The existence of limit cycles is studied by the method of *Poincaré sections* (Poincaré 1882, “Chap. V, Théorie des conséquents”). The idea is to cut the solutions transversally by a hyperplane Π and, for an initial value $y_0 \in \Pi$, to study the first point $\Phi(y_0)$ where the solution again crosses the plane Π in the same direction.

For our example (16.2), we choose for Π the half-line $y_2 = 0$, $y_1 > 0$. We then examine the signs of y'_1 and y'_2 in (16.2). The sign of y'_2 changes at the curve

$$y_2 = \frac{y_1}{\epsilon(1-y_1^2)}, \quad (16.3)$$

which is drawn as a broken line in Fig. 16.2. It follows (see Fig. 16.2) that $\Phi(y_0)$ exists for all $y_0 \in \Pi$. Since two different solutions *cannot intersect* (due to uniqueness), the map Φ is *monotone*. Further, Φ is bounded (e.g., by every solution starting on the curve (16.3)), so $\Phi(y_0) < y_0$ for y_0 large. Finally, since the origin is unstable, $\Phi(y_0) > y_0$ for y_0 small. Hence there must be a fixed point of $\Phi(y_0)$, i.e., a limit cycle. \square

The limit cycle is, in fact, *unique*. The proof for this is more complicated and is indicated in Exercise 8 below (Liénard 1928).

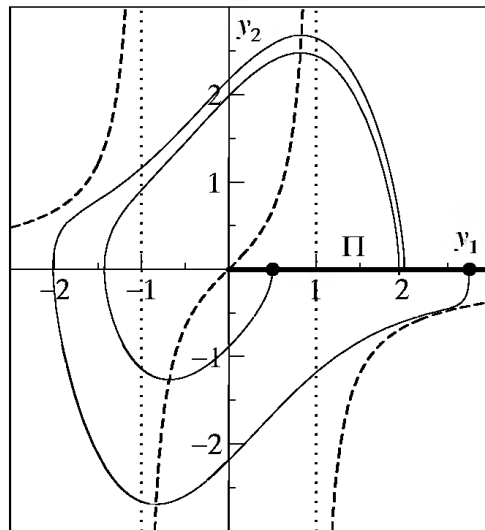


Fig. 16.2. The Poincaré map for Van der Pol's equation, $\varepsilon = 1$

With similar ideas one proves the following general result:

Theorem 16.1 (Poincaré 1882, Bendixson 1901). *Each bounded solution of a two-dimensional system*

$$y'_1 = f_1(y_1, y_2), \quad y'_2 = f_2(y_1, y_2) \quad (16.4)$$

must

- i) tend to a critical point $f_1 = f_2 = 0$ for an infinity of points $x_i \rightarrow \infty$; or
- ii) be periodic; or
- iii) tend to a limit cycle. □

Remark. Exercise 1 below explains why the possibility (i) is written in a form somewhat more complicated than seems necessary.

Steady-state approximations for ε large. An important tool for simplifying complicated nonlinear systems is that of steady-state approximations. Consider (16.2) with ε very large. Then, in the neighbourhood of $f_2(y_1, y_2) = 0$ for $|y_1| > 1$, the derivative of $y'_2 = f_2$ with respect to y_2 is very large negative. Therefore the solution will very rapidly approach an equilibrium state in the neighbourhood of $y'_2 = f_2(y_1, y_2) = 0$, i.e., in our example, $y_2 = y_1 / (\varepsilon(1 - y_1^2))$. This can be inserted into (16.2) and leads to

$$y'_1 = \frac{y_1}{\varepsilon(1 - y_1^2)}, \quad (16.5)$$

an equation of lower dimension. Using the formulas of Section I.3, (16.5) is easily

solved to give

$$\log(y_1) - \frac{y_1^2}{2} = \frac{x - x_0}{\varepsilon} + \text{Const.}$$

These curves are dotted in Van der Pol's Fig. 16.3 for $\varepsilon = 10$ and show the good approximation of this solution.

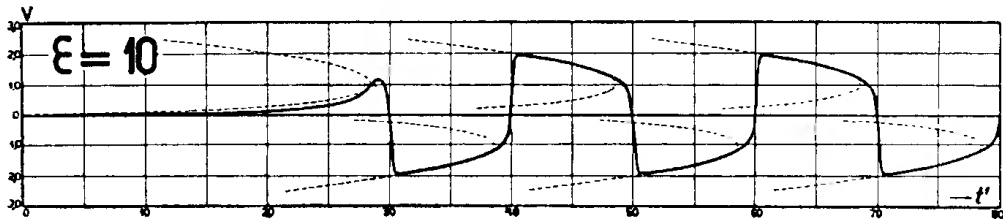


Fig. 16.3. Solution of Van der Pol's equation for $\varepsilon = 10$
compared with steady state approximations

Asymptotic solutions for ε small. The computation of periodic solutions for *small* parameters was initiated by astronomers such as Newcomb and Lindstedt and brought to perfection by Poincaré (1893). We demonstrate the method for the Van der Pol equation (16.1). The idea is to develop the solution as a series in powers of ε . Since the period will change too, we also introduce a coordinate change

$$t = x(1 + \gamma_1\varepsilon + \gamma_2\varepsilon^2 + \dots) \quad (16.6)$$

and put

$$y(x) = z(t) = z_0(t) + \varepsilon z_1(t) + \varepsilon^2 z_2(t) + \dots \quad (16.7)$$

Inserting now $y'(x) = z'(t)(1 + \gamma_1\varepsilon + \dots)$, $y''(x) = z''(t)(1 + \gamma_1\varepsilon + \dots)^2$ into (16.1) we obtain

$$\begin{aligned} & (z_0'' + \varepsilon z_1'' + \varepsilon^2 z_2'' + \dots)(1 + 2\gamma_1\varepsilon + (2\gamma_2 + \gamma_1^2)\varepsilon^2 + \dots) \\ & + \varepsilon((z_0 + \varepsilon z_1 + \dots)^2 - 1)(z_0' + \varepsilon z_1' + \dots)(1 + \gamma_1\varepsilon + \dots) \\ & + (z_0 + \varepsilon z_1 + \varepsilon^2 z_2 + \dots) = 0. \end{aligned} \quad (16.8)$$

We first compare the coefficients of ε^0 and obtain

$$z_0'' + z_0 = 0. \quad (16.8;0)$$

We fix the initial value on the Poincaré section P , i.e., $z'(0) = 0$, so that $z_0 = A \cos t$ with A , for the moment, a free parameter. Next, the coefficients of ε yield

$$\begin{aligned} z_1'' + z_1 &= -2\gamma_1 z_0'' - (z_0^2 - 1)z_0' \\ &= 2\gamma_1 A \cos t + \left(\frac{A^3}{4} - A\right) \sin t + \frac{A^3}{4} \sin 3t. \end{aligned} \quad (16.8;1)$$

Here, the crucial idea is that we are looking for *periodic* solutions, hence the terms in $\cos t$ and $\sin t$ on the right-hand side of (16.8;1) must disappear, in order to avoid that $z_1(t)$ contain terms of the form $t \cdot \cos t$ and $t \cdot \sin t$ (“... et de faire disparaître ainsi les termes dits *séculaires* ...”). We thus obtain $\gamma_1 = 0$ and $A = 2$. Then (16.8;1) can be solved and gives, together with $z'_1(0) = 0$,

$$z_1 = B \cos t + \frac{3}{4} \sin t - \frac{1}{4} \sin 3t. \quad (16.9)$$

The continuation of this process is now clear: the terms in ε^2 in (16.8) lead to, after insertion of (16.9) and simplification,

$$z''_2 + z_2 = \left(4\gamma_2 + \frac{1}{4}\right) \cos t + 2B \sin t + 3B \sin 3t - \frac{3}{2} \cos 3t + \frac{5}{4} \cos 5t. \quad (16.8;2)$$

Secular terms are avoided if we set $B = 0$ and $\gamma_2 = -1/16$. Then

$$z_2 = C \cos t + \frac{3}{16} \cos 3t - \frac{5}{96} \cos 5t.$$

The next round will give $C = -1/8$ and $\gamma_3 = 0$, so that we have: *the periodic orbit of the Van der Pol equation (16.1) for ε small is given by*

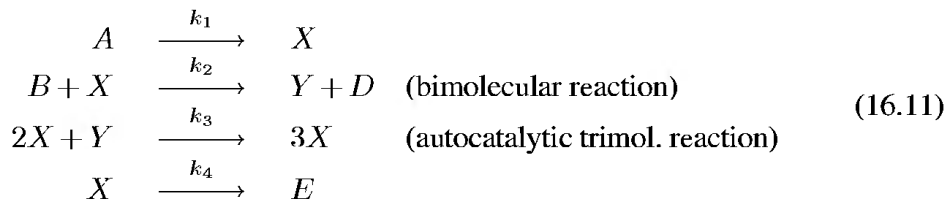
$$\begin{aligned} y(x) &= z(t), \quad t = x(1 - \varepsilon^2/16 + \dots), \\ z(t) &= 2 \cos t + \varepsilon \left(\frac{3}{4} \sin t - \frac{1}{4} \sin 3t \right) \\ &\quad + \varepsilon^2 \left(-\frac{1}{8} \cos t + \frac{3}{16} \cos 3t - \frac{5}{96} \cos 5t \right) + \dots \end{aligned} \quad (16.10)$$

and is of period $2\pi(1 + \varepsilon^2/16 + \dots)$.

Chemical Reactions

The laws of chemical kinetics give rise to differential equations which, for multi-molecular reactions, become nonlinear and have interesting properties. Some of them possess periodic solutions (e.g. the Zhabotinski-Belousov reaction) and have important applications to the interpretation of biological phenomena (e.g. Prigogine, Lefever).

Let us examine in detail the model of Lefever and Nicolis (1971), the so-called “Brusselator”: suppose that six substances A, B, D, E, X, Y undergo the following reactions:



If we denote by $A(x), B(x), \dots$ the *concentrations* of A, B, \dots as functions of the time x , the reactions (16.11) become by the mass action law the following differential equations

$$\begin{aligned} A' &= -k_1 A \\ B' &= -k_2 BX \\ D' &= k_2 BX \\ E' &= k_4 X \\ X' &= k_1 A - k_2 BX + k_3 X^2 Y - k_4 X \\ Y' &= k_2 BX - k_3 X^2 Y. \end{aligned}$$

This system is now simplified as follows: the equations for D and E are left out, because they do not influence the others; A and B are supposed to be maintained constant (positive) and all reaction rates k_i are set equal to 1. We further set $y_1(x) := X(x)$, $y_2(x) := Y(x)$ and obtain

$$\begin{aligned} y'_1 &= A + y_1^2 y_2 - (B + 1)y_1 \\ y'_2 &= B y_1 - y_1^2 y_2. \end{aligned} \tag{16.12}$$

The resulting system has one critical point $y'_1 = y'_2 = 0$ at $y_1 = A$, $y_2 = B/A$. The linearized equation in the neighbourhood of this point is unstable iff $B > A^2 + 1$. Further, a study of the domains where y'_1 , y'_2 , or $(y_1 + y_2)'$ is positive or negative leads to the result that all solutions remain bounded. Thus, for $B > A^2 + 1$ there must be a limit cycle which, by numerical calculations, is seen to be unique (Fig. 16.4).

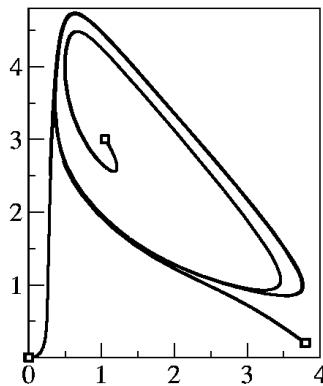


Fig. 16.4. Solutions of the Brusselator, $A = 1$, $B = 3$

An interesting phenomenon (Hopf bifurcation, see below) occurs, when B approaches $A^2 + 1$. Then the limit cycle becomes smaller and smaller and finally disappears in the critical point. Another example of this type is given in Exercise 2.

Limit Cycles in Higher Dimensions, Hopf Bifurcation

The Theorem of Poincaré-Bendixson is apparently true only in two dimensions. Higher dimensional counter-examples are given by nearly every mechanical movement without friction, as for example the spherical pendulum (6.20), see Fig. 6.2. Therefore, in higher dimensions limit cycles are usually found by numerical studies of the Poincaré section map Φ defined above.

There is, however, one situation where limit cycles occur quite naturally (Hopf 1942): namely when at a critical point of $y' = f(y, \alpha)$, $y, f \in \mathbb{R}^n$, all eigenvalues of $(\partial f / \partial y)(y_0, \alpha)$ have strictly negative real part with the exception of *one* pair which, by varying α , crosses the imaginary axis. The eigenspace of the stable eigenvalues then continues into an analytic two dimensional manifold, inside which a limit cycle appears. This phenomenon is called “Hopf bifurcation”. The proof of this fact is similar to Poincaré’s parameter expansion method (16.7) (see Exercises 6 and 7 below), so that Hopf even hesitated to publish it (“... ich glaube kaum, dass an dem obigen Satz etwas wesentlich Neues ist ...”).

As an example, we consider the “full Brusselator” (16.11): we no longer suppose that B is kept constant, but that B is constantly added to the mixture with

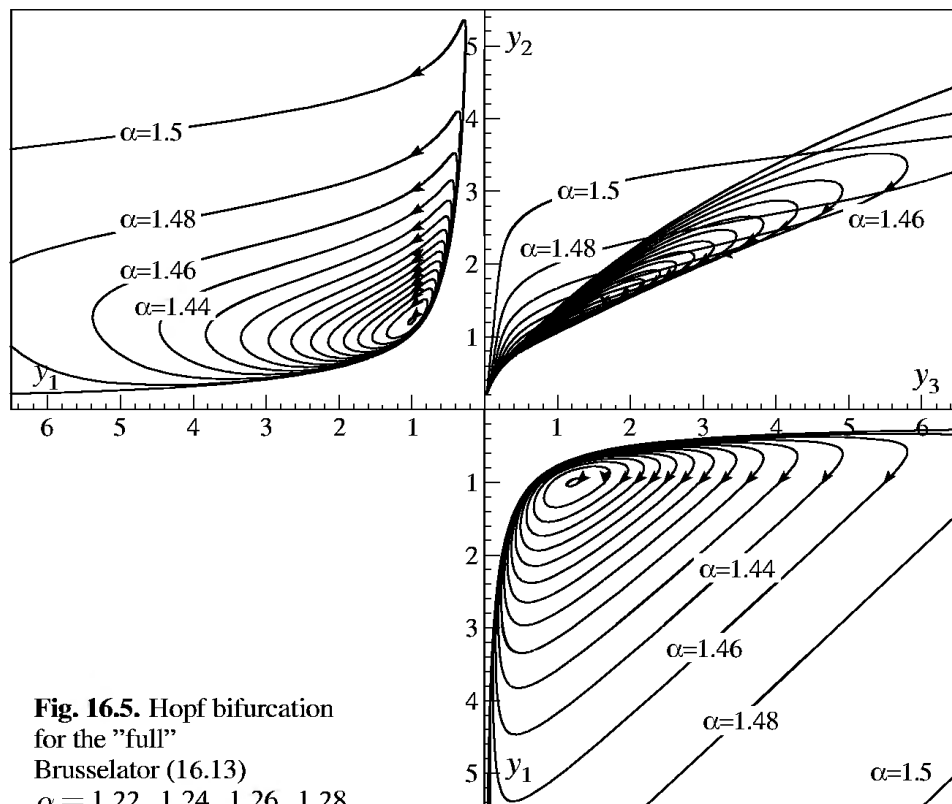


Fig. 16.5. Hopf bifurcation for the "full" Brusselator (16.13)
 $\alpha = 1.22, 1.24, 1.26, 1.28, \dots$

rate α . When we set $y_3(x) := B(x)$, we obtain instead of (16.12) (with $A = 1$)

$$\begin{aligned} y'_1 &= 1 + y_1^2 y_2 - (y_3 + 1)y_1 \\ y'_2 &= y_1 y_3 - y_1^2 y_2 \\ y'_3 &= -y_1 y_3 + \alpha. \end{aligned} \quad (16.13)$$

This system possesses a critical point at $y_1 = 1$, $y_2 = y_3 = \alpha$ with derivative

$$\frac{\partial f}{\partial y} = \begin{pmatrix} \alpha - 1 & 1 & -1 \\ -\alpha & -1 & 1 \\ -\alpha & 0 & -1 \end{pmatrix}. \quad (16.14)$$

This matrix has $\lambda^3 + (3 - \alpha)\lambda^2 + (3 - 2\alpha)\lambda + 1$ as characteristic polynomial and satisfies the condition for stability iff $\alpha < (9 - \sqrt{17})/4 = 1.21922$ (see I.13, Exercise 1). Thus when α increases beyond this value, there arises a limit cycle which exists for all values of α up to approximately 1.5 (see Fig. 16.5). When α continues to grow, the limit cycle “explodes” and $y_1 \rightarrow 0$ while y_2 and $y_3 \rightarrow \infty$. So the system (16.13) has a behaviour completely different from the simplified model (16.12).

A famous chemical reaction with a limit cycle in three dimensions is the “Oreg-onator” reaction between $HBrO_2$, Br^- , and $Ce(IV)$ (Field & Noyes 1974)

$$\begin{aligned} y'_1 &= 77.27 \left(y_2 + y_1 (1 - 8.375 \times 10^{-6} y_1 - y_2) \right) \\ y'_2 &= \frac{1}{77.27} (y_3 - (1 + y_1) y_2) \\ y'_3 &= 0.161 (y_1 - y_3) \end{aligned} \quad (16.15)$$

whose solutions are plotted in Fig. 16.6. This is an example of a “stiff” differential equation whose solutions change rapidly over many orders of magnitude. It is thus a challenging example for numerical codes and we shall meet it again in Volume II of our book.

Our next example is taken from the theory of superconducting Josephson junctions, coupled together by a mutual capacitance. Omitting all physical details, (see Giovannini, Weiss & Ulrich 1978), we state the resulting equations as

$$\begin{aligned} c(y''_1 - \alpha y''_2) &= i_1 - \sin(y_1) - y'_1 \\ c(y''_2 - \alpha y''_1) &= i_2 - \sin(y_2) - y'_2. \end{aligned} \quad (16.16)$$

Here, y_1 and y_2 are *angles* (the “quantum phase difference across the junction”) which are thus identified modulo 2π . Equation (16.16) is thus a system on the torus T^2 for (y_1, y_2) , and on \mathbb{R}^2 for the voltages (y'_1, y'_2) . It is seen by numerical computations that the system (16.16) possesses an attracting limit cycle, which describes the phenomenon of “phase locking” (see Fig. 16.7).

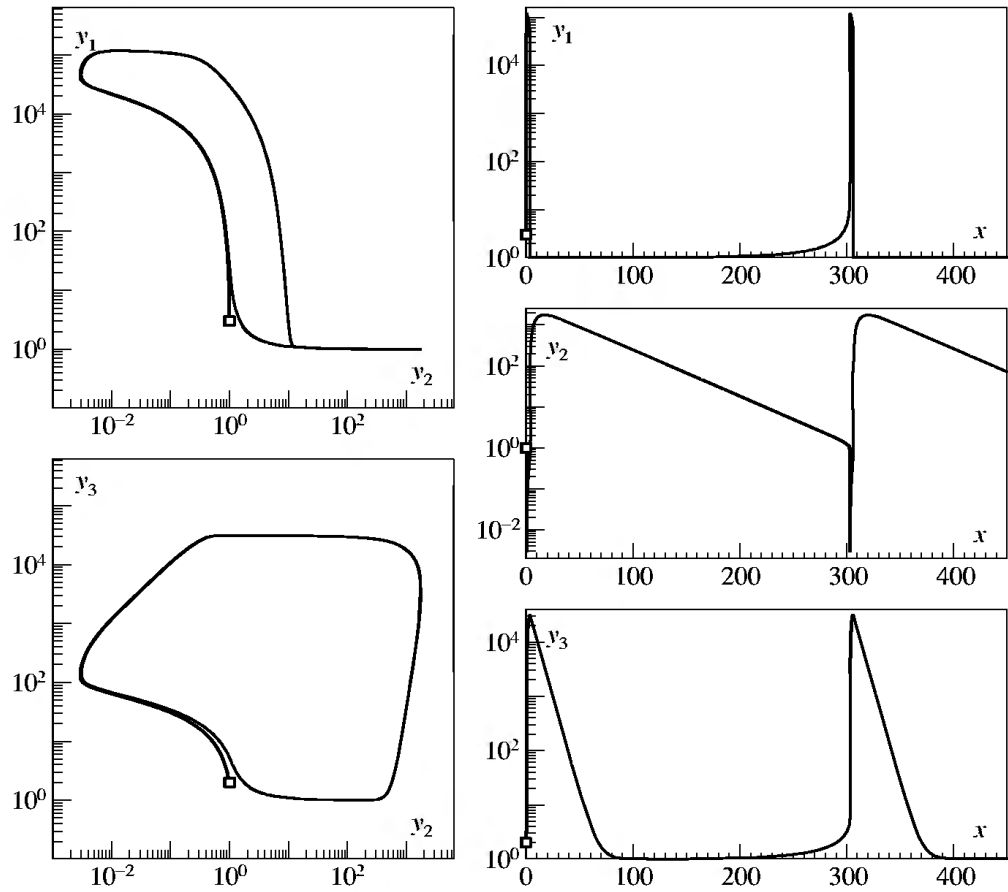


Fig. 16.6. Limit cycle of the Oregonator

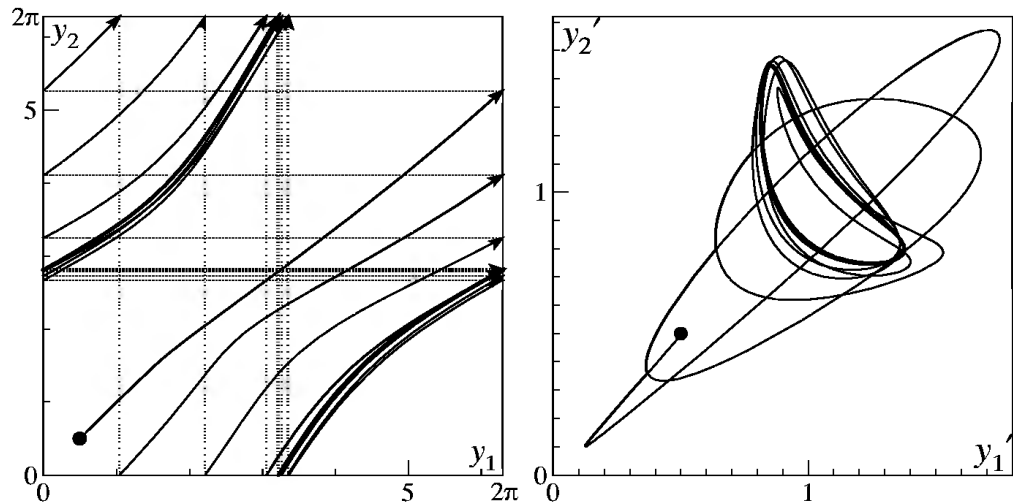


Fig. 16.7. Josephson junctions (16.16) for $c = 2$, $\alpha = 0.5$, $i_1 = 1.11$, $i_2 = 1.08$

Strange Attractors

“Mr. Dahlquist, when is the spring coming ?”

“Tomorrow, at two o’clock.”

(Weather forecast, Stockholm 1955)

“We were **so** naïve . . .”

(H.O. Kreiss, Stockholm 1985)

Concerning the discovery of the famous “Lorenz model”, we best quote from Lorenz (1979):

“By the middle 1950’s “numerical weather prediction”, i.e., forecasting by numerically integrating such approximations to the atmospheric equations as could feasibly be handled, was very much in vogue, despite the rather mediocre results which it was then yielding. A smaller but determined group favored statistical prediction (...) apparently because of a misinterpretation of a paper by Wiener (...). I was skeptical, and decided to test the idea by applying the statistical method to a set of artificial data, generated by solving a system of equations numerically (...). The first task was to find a suitable system of equations to solve (...). The system would have to be simple enough (...) and the general solution would have to be aperiodic, since the statistical prediction of a periodic series would be a trivial matter, once the periodicity had been detected. It was not obvious that these conditions could be met. (...) The break came when I was visiting Dr. Barry Saltzman, now at Yale University. In the course of our talks he showed me some work on thermal convection, in which he used a system of seven ordinary differential equations. Most of his numerical solutions soon acquired periodic behavior, but one solution refused to settle down. Moreover, in this solution four of the variables appeared to approach zero. Presumably the equations governing the remaining three variables, with the terms containing the four variables eliminated, would also possess aperiodic solutions. Upon my return I put the three equations on our computer, and confirmed the aperiodicity which Saltzman had noted. We were finally in business.”

In a changed notation, the three equations with aperiodic solutions are

$$\begin{aligned} y'_1 &= -\sigma y_1 + \sigma y_2 \\ y'_2 &= -y_1 y_3 + r y_1 - y_2 \\ y'_3 &= y_1 y_2 - b y_3 \end{aligned} \tag{16.17}$$

where σ , r and b are positive constants. It follows from (16.17) that

$$\begin{aligned} \frac{1}{2} \frac{d}{dx} \left(y_1^2 + y_2^2 + (y_3 - \sigma - r)^2 \right) \\ = - \left(\sigma y_1^2 + y_2^2 + b(y_3 - \frac{\sigma}{2} - \frac{r}{2})^2 \right) + b \left(\frac{\sigma}{2} + \frac{r}{2} \right)^2. \end{aligned} \tag{16.18}$$

Therefore the ball

$$R_0 = \left\{ (y_1, y_2, y_3) \mid y_1^2 + y_2^2 + (y_3 - \sigma - r)^2 \leq c^2 \right\} \quad (16.19)$$

is mapped by the flow φ_1 (see (14.22)) into itself, provided that c is sufficiently large so that R_0 wholly contains the ellipsoid defined by equating the right side of (16.18) to zero. Hence, if x assumes the increasing values $1, 2, 3, \dots$, R_0 is carried into regions $R_1 = \varphi_1(R_0)$, $R_2 = \varphi_2(R_0)$ etc., which satisfy $R_0 \supset R_1 \supset R_2 \supset R_3 \supset \dots$ (applying φ_1 to the inclusion $R_0 \supset R_1$ gives $R_1 \supset R_2$ and so on).

Since the trace of $\partial f / \partial y$ for the system (16.17) is the negative constant $-(\sigma + b + 1)$, the volumes of R_k tend exponentially to zero (see Theorem 14.8). Every orbit is thus ultimately trapped in a set $R_\infty = R_0 \cap R_1 \cap R_2 \dots$ of zero volume.

System (16.17) possesses an obvious critical point $y_1 = y_2 = y_3 = 0$; this becomes unstable when $r > 1$. In this case there are two additional critical points C and C' respectively given by

$$y_1 = y_2 = \pm \sqrt{b(r-1)}, \quad y_3 = r-1. \quad (16.20)$$

These become unstable (e.g. by the Routh criterion, Exercise 1 of Section I.13) when $\sigma > b + 1$ and

$$r \geq r_c = \frac{\sigma(\sigma + b + 3)}{\sigma - b - 1}. \quad (16.21)$$

In the first example we shall use Saltzman's values $b = 8/3$, $\sigma = 10$, and $r = 28$. ("Here we note another lucky break: Saltzman used $\sigma = 10$ as a crude approximation to the Prandtl number (about 6) for water. Had he chosen to study air, he would probably have let $\sigma = 1$, and the aperiodicity would not have been discovered", Lorenz 1979). In Fig. 16.8 we have plotted the solution curve of (16.17) with the initial value $y_1 = -8$, $y_2 = 8$, $y_3 = r - 1$, which, indeed, looks pretty chaotic.

For a clearer understanding of the phenomenon, we choose the plane $y_3 = r - 1$, especially the square region between the critical points C and C' , as Poincaré section Π . The critical point $y_1 = y_2 = y_3 = 0$ possesses (since $r > 1$) one unstable eigenvalue $\lambda_1 = (-1 - \sigma + \sqrt{(1 - \sigma)^2 + 4r\sigma})/2$ and two stable eigenvalues $\lambda_2 = -b$, $\lambda_3 = (-1 - \sigma - \sqrt{(1 - \sigma)^2 + 4r\sigma})/2$. The eigenspace of the stable eigenvalues continues into a two-dimensional manifold of initial values, whose solutions tend to 0 for $x \rightarrow \infty$. This "stable manifold" cuts Π in a curve Σ (see Fig. 16.9). The one-dimensional *unstable* manifold (created by the unstable eigenvalue λ_1) cuts Π in the points D and D' (Fig. 16.9).

All solutions starting in Π_u above Σ (the dark cat) surround the above critical point C and are, at the first return, mapped to a narrow stripe S_u , while the solutions starting in Π_d below Σ surround C' and go to the left stripe S_d . At the second return, the two stripes are mapped into two very narrow stripes *inside* S_u and S_d . After the third return, we have 8 stripes closer and closer together, and so on. The intersection of all these stripes is a Cantor-like set and, continued

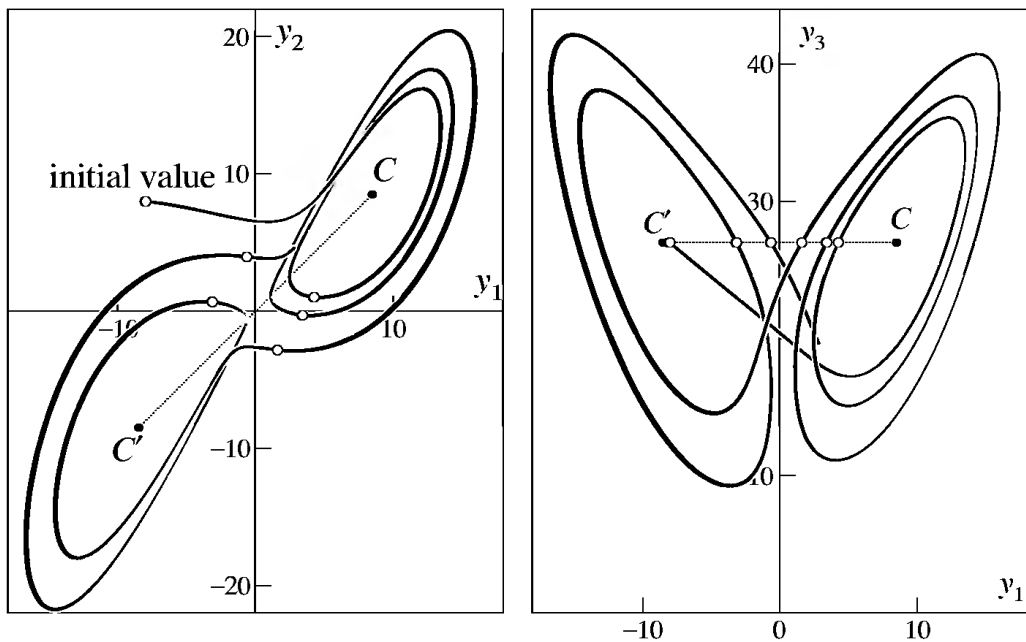


Fig. 16.8. Two views of a solution of (16.17)
(small circles indicate intersection of solution with plane $y_3 = r - 1$)

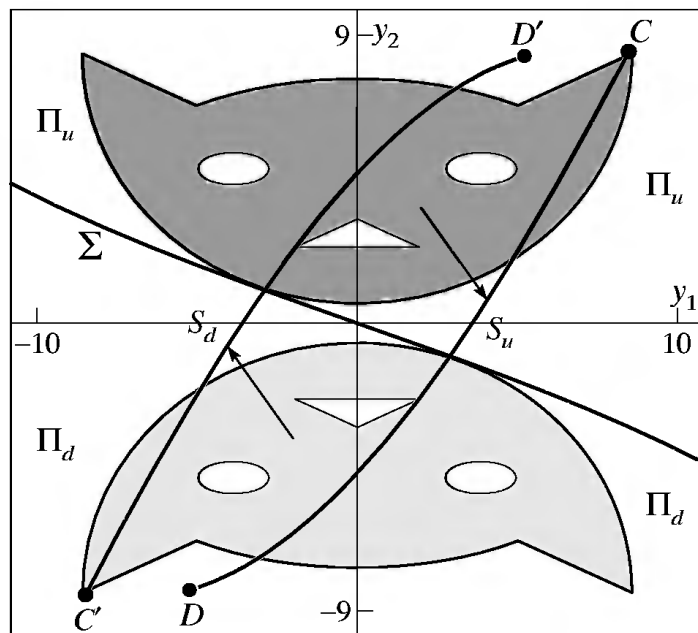
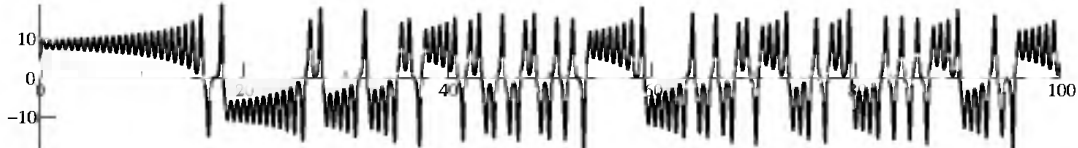


Fig. 16.9. Poincaré map for (16.17)

into 3-space by the flow, forms the *strange attractor* (“An attractor of the type just described can therefore not be thrown away as non-generic pathology”, Ruelle & Takens 1971).

The Ups and Downs of the Lorenz Model

“Mr. Laurel and Mr. Hardy have many ups and downs — Mr. Hardy takes charge of the upping, and Mr. Laurel does most of the downing —”
 (from “Another Fine Mess”, Hal Roach 1930)



If one watches the solution $y_1(x)$ of the Lorenz equation being calculated, one wonders who decides for the solution to go up or down in an apparently unpredictable fashion. Fig. 16.9 shows that Σ cuts both stripes S_d and S_u . Therefore the *inverse image* of Σ (see Fig. 16.10) consists of two lines Σ_0 and Σ_1 which cut, together with Σ , the plane Π into four sets Π_{uu} , Π_{ud} , Π_{du} , Π_{dd} . If the initial value is in one of these, the corresponding solution goes up-up, up-down, down-up, down-down. Further, the inverse images of Σ_0 and Σ_1 lead to four lines Σ_{00} , Σ_{01} , Σ_{10} , Σ_{11} . The plane Π is then cut into 8 stripes and we now know the fate of the first three ups and downs. The more inverse images of these curves we compute, the finer the plane Π is cut into stripes and all the future ups and downs are coded in the position of the initial value with respect to these stripes (see Fig. 16.10). It appears that a *very small* change in the initial value gives rise, after a couple of rotations, to a *totally different* solution curve. This phenomenon, discovered merely by accident by Lorenz (see Lorenz 1979), is highly interesting

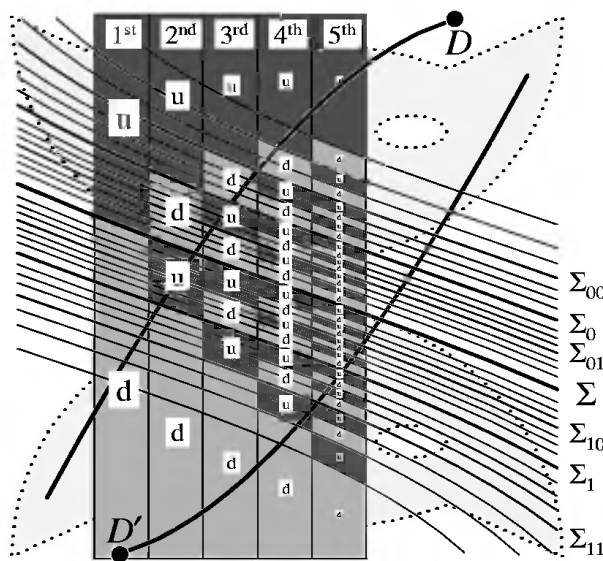


Fig. 16.10. Stripes deciding for the ups and downs

and explains why the theorem of uniqueness (Theorem 7.4), of whose philosophical consequences Laplace was so proud, has its practical limits.

Remark. It appears in Fig. 16.10 that not all stripes have the same width. The sequences of “*u*”’s and “*d*”’s which repeat *u* or *d* a couple of times (but not too often) are more probable than the others. More than 25 consecutive “ups” or “downs” are (for the chosen constants and except for the initial phase) never possible. This has to do with the position of *D* and *D'*, the outermost frontiers of the attractor, in the stripes of Fig. 16.10.

Feigenbaum Cascades

However nicely the beginning of Lorenz’ (1979) paper is written, the affirmations of his last section are only partly true. As Lorenz did, we now vary the parameter *b* in (16.17), letting at the same time $r = r_c$ (see (16.21)) and

$$\sigma = b + 1 + \sqrt{2(b+1)(b+2)}. \quad (16.22)$$

This is the value of σ for which r_c is minimized. Numerical integration shows that for *b* very small (say $b \leq 0.139$), the solutions of (16.17) evidently converge to a stable limit cycle, which cuts the Poincaré section $y_3 = r - 1$ twice at two different locations and surrounds both critical points *C* and *C'*. Further, for *b* large (for example $b = 8/3$) the coefficients are not far from those studied above and we have a strange attractor. But what happens in between? We have computed the solutions of the Lorenz model (16.17) for *b* varying from 0.1385 to 0.1475 with 1530 intermediate values. For each of these values, we have computed 1500 Poincaré cuts and represented in Fig. 16.11 the y_1 -values of the intersections with the Poincaré plane $y_3 = r - 1$. After each change of *b*, the first 300 iterations were not drawn so that only the attractor becomes visible.

For *b* small, there is one periodic orbit; then, at $b = b_1 = 0.13972$, it suddenly splits into an orbit of period two, this then splits for $b = b_2 = 0.14327$ into an orbit of period four, then for $b = b_3 = 0.14400$ into period eight, etc. There is a point $b_\infty = 0.14422$ after which the movement becomes chaotic. Beyond this value, however, there are again and again intervals of stable attractors of periods 5, 3, etc. The whole picture resembles what is obtained by the recursion

$$x_{n+1} = a(x_n - x_n^2) \quad (16.23)$$

which is discussed in many papers (e.g. May 1976, Feigenbaum 1978, Collet & Eckmann 1980).

But where does this resemblance come from? We study in Fig. 16.12 the Poincaré map for the system (16.17) with *b* chosen as 0.146 of a region $-0.095 \leq y_1 \leq -0.078$ and $-0.087 \leq y_2 \leq -0.07$. After one return, this region is compressed to a thin line somewhere else on the plane (Fig. 16.12b), the second return bends this line to *U*-shape and maps it into the original region (Fig. 16.12c).

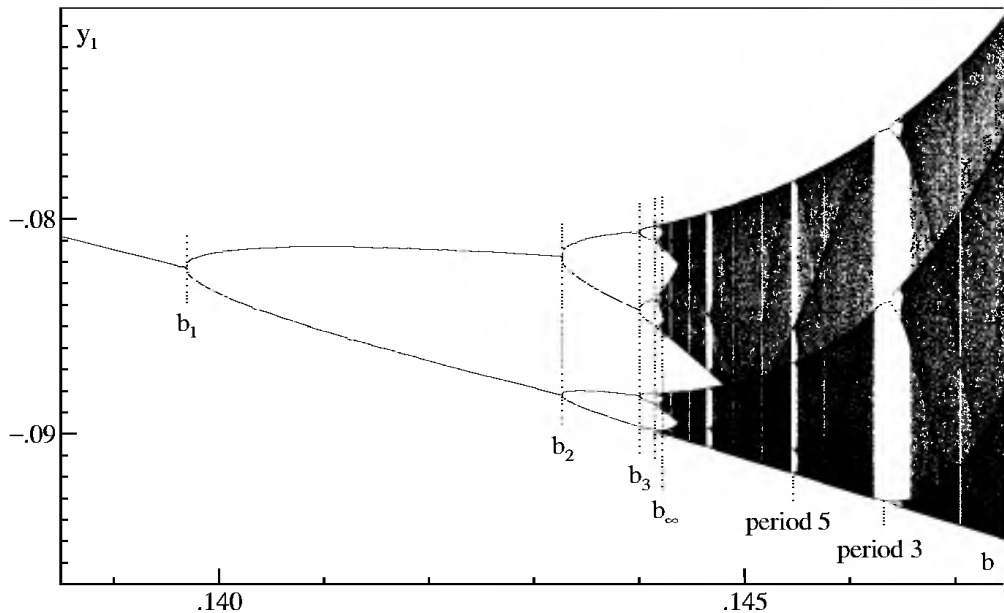


Fig. 16.11. Poincaré cuts y_1 for (16.17) as function of b

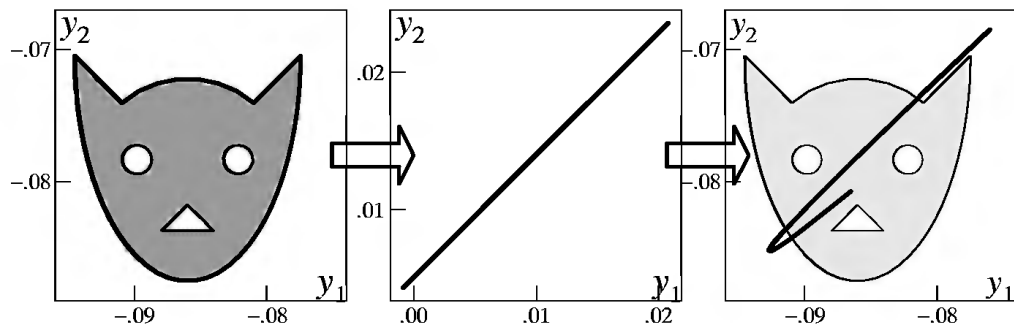


Fig. 16.12. Poincaré map for system (16.17) with $b = 0.146$

Therefore, the Poincaré map is essentially a map of the interval $[0, 1]$ to itself similar to (16.23). It is a great discovery of Feigenbaum that for *all* maps of a similar shape, the phenomena are always the same, in particular that

$$\lim_{i \rightarrow \infty} \frac{b_i - b_{i-1}}{b_{i+1} - b_i} = 4.6692016091029906715\dots$$

is a universal constant, the *Feigenbaum number*. The repeated doublings of the periods at b_1, b_2, b_3, \dots are called *Feigenbaum cascades*.

Exercises

1. The Van der Pol equation (16.2) with $\varepsilon = 1$ possesses a limit cycle of period $T = 6.6632868593231301896996820305$ passing through $y_2 = 0$, $y_1 = A$ where $A = 2.00861986087484313650940188$. Replace (16.2) by

$$\begin{aligned} y'_1 &= y_2(A - y_1) \\ y'_2 &= ((1 - y_1^2)y_2 - y_1)(A - y_1) \end{aligned}$$

so that the limit cycle receives a stationary point. Study the behaviour of a solution starting in the interior, e.g. at $y_{10} = 1$, $y_{20} = 0$.

2. (Frommer 1934). Consider the system

$$y'_1 = -y_2 + 2y_1y_2 - y_2^2, \quad y'_2 = y_1 + (1 + \varepsilon)y_1^2 + 2y_1y_2 - y_2^2. \quad (16.24)$$

Show, either by a stability analysis similar to Exercise 5 of Section I.13 or by numerical computations, that for $\varepsilon > 0$ (16.24) possesses a limit cycle of asymptotic radius $r = \sqrt{6\varepsilon/7}$. (See also Wanner (1983), p. 15 and I.13, Exercise 5).

3. Solve Hilbert's 16th Problem: what is the highest possible number of limit cycles that a quadratic system

$$\begin{aligned} y'_1 &= \alpha_0 + \alpha_1y_1 + \alpha_2y_2 + \alpha_3y_1^2 + \alpha_4y_1y_2 + \alpha_5y_2^2 \\ y'_2 &= \beta_0 + \beta_1y_1 + \beta_2y_2 + \beta_3y_1^2 + \beta_4y_1y_2 + \beta_5y_2^2 \end{aligned}$$

can have? The mathematical community is waiting for *you*: nobody has been able to solve this problem for more than 80 years. At the moment, the highest known number is 4, as for example in the system

$$\begin{aligned} y'_1 &= \lambda y_1 - y_2 - 10y_1^2 + (5 + \delta)y_1y_2 + y_2^2 \\ y'_2 &= y_1 + y_1^2 + (-25 + 8\varepsilon - 9\delta)y_1y_2, \\ \delta &= -10^{-13}, \quad \varepsilon = -10^{-52}, \quad \lambda = -10^{-200} \end{aligned}$$

(see Shi Songling 1980, Wanner 1983, Perko 1984).

4. Find a change of coordinates such that the equation

$$my'' + (-A + B(y')^2)y' + ky = 0$$

becomes the Van der Pol equation (16.2) (see Kryloff & Bogoliuboff (1947), p. 5).

5. Treat the pendulum equation

$$y'' + \sin y = y'' + y - \frac{y^3}{6} + \frac{y^5}{120} \pm \dots = 0, \quad y(0) = \varepsilon, \quad y'(0) = 0,$$

by the method of asymptotic expansions (16.6) and (16.7) and study the period as a function of ε .

Result. The period is $2\pi(1 + \varepsilon^2/16 + \dots)$.

6. Compute the limit cycle (Hopf bifurcation) for

$$y'' + y = \varepsilon^2 y' - (y')^3$$

for ε small by the method of Poincaré (16.6), (16.7) with $z'(0) = 0$.

7. Treat in a similar way as in Exercise 6 the Brusselator (16.12) with $A = 1$ and $B = 2 + \varepsilon^2$.

Hint. With the new variable $y = y_1 + y_2 - 3$ the differential equation (16.12) becomes equivalent to $y' = 1 - y_1$ and

$$y'' + y = -\varepsilon^2(y' - 1) - (y')^2(y + y') + 2yy'.$$

Result. $z(t) = \varepsilon(2/\sqrt{3}) \cos t + \dots$, $t = x(1 - \varepsilon^2/18 + \dots)$, so that the period is asymptotically $2\pi(1 + \varepsilon^2/18 + \dots)$.

8. (Liénard 1928). Prove that the limit cycle of the Van der Pol equation (16.1) is unique for every $\varepsilon > 0$.

Hint. The identity

$$y'' + \varepsilon(y^2 - 1)y' = \frac{d}{dx} \left(y' + \varepsilon \left(\frac{y^3}{3} - y \right) \right)$$

suggests the use of the coordinate system $y_1(x) = y(x)$, $y_2(x) = y' + \varepsilon(y^3/3 - y)$. Write the resulting first order system, study the signs of y'_1 , y'_2 and the increase of the “energy” function $V(x) = (y_1^2 + y_2^2)/2$.

Also generalize the result to equations of the form $y'' + f(y)y' + g(y) = 0$. For more details see e.g. Simmons (1972), p. 349.

9. (Rayleigh 1883). Compute the periodic solution of

$$y'' + \kappa y' + \lambda(y')^3 + n^2 y = 0$$

for κ and λ small.

Result. $y = A \sin(nx) + (\lambda n A^3/32) \cos(3nx) + \dots$ where A is given by $\kappa + (3/4)\lambda n^2 A^2 = 0$.

10. (Bendixson 1901). If in a certain region Ω of the plane the expression

$$\frac{\partial f_1}{\partial y_1} + \frac{\partial f_2}{\partial y_2}$$

is always negative or always positive, then the system (16.4) cannot have closed solutions in Ω .

Hint. Apply Green's formula

$$\int \int \left(\frac{\partial f_1}{\partial y_1} + \frac{\partial f_2}{\partial y_2} \right) dy_1 dy_2 = \int (f_1 dy_2 - f_2 dy_1).$$